Identification of the Precipitates by TEM and EDS in X20CrMoV12.1 After Long-Term Service at Elevated Temperature

Hu Zheng-Fei and Yang Zhen-Guo

(Submitted 26 April 2002; in revised form 1 October 2002)

The crystal structures, morphologies, and compositions of carbides in a martensitic pipe steel of type X20CrMoV12.1 after long-term service at 550 °C have been carefully investigated using transmission electron microscopy (TEM) and dispersive x-ray spectrometry (EDS). Most of carbides are $M_{23}C_6$. The $M_{23}C_6$ particles in prior austenite grains and in martensite lath boundaries are extensively coarsened. Most of the finer carbides within the matrix are also identified as $M_{23}C_6$, and no other type of carbide was found except for some tiny plate-like V-rich carbides identified as MC. The V and O mass fractions in the $M_{23}C_6$ carbides have variable morphologies and locations, which might be due to their coarsening process. They are coarsening at different rates even after long-term exposure at elevated temperature. The formation of V-rich MC during the long-term service contributes to hardness maintenance and is good for microstructural stability.

Keywords aging, carbide morphology, chromium steel, steel, X20CrMoV12.1

1. Introduction

In the past decades, the 9-12% Cr martensitic steels have been widely used as pipework and tubing in the power-generating industry around the world. To understand the mechanical properties of the materials and their behavior in practical applications, many investigations have undertaken creep or fatigue tests on materials before and after long-term service.[1-3] One of the 12CrMoV steels, standardized for use in steam pipes under the German standard DIN17175 designation, is X20CrMoV12.1, which has been widely used for steam pipes in power plants since the 1960s in Europe and other countries. Some of the steam pipes have been in service more than 20 years, and their mechanical properties and microstructures have degraded. To evaluate or prolong the service time of those steam pipes, it is important to examine their mechanical behavior and microstructural stability. Some of the investigations[3,4] for X20CrMoV12.1 steam pipes indicated that severe softening did not occur after long-term service exposure at elevated temperature. A particularly important aspect of the microstructure is the distribution of carbide particles.[5] Some work on 12CrMoV pipe steels indicated that the carbides of $M_{23}C_6$, M_7C_3, M_2X, and MX (M denotes the metal elements, and X denotes non-metallic elements of C and N) were found in their as-received heat treatment or after creep exposure test conditions, which were believed to be decisive factors for precipitation hardening, as well as high creep strength.[6-8] In the past, much more attention was paid to the coarsening of carbides in boundaries; however, the morphologies and characteristics of the carbides in the matrix have not been well reported and identified.

This article describes detailed results of transmission electron microscopy (TEM) and dispersive x-ray spectrometer (EDS) investigation studies of the morphologies and compositional changes of carbides in a main steam pipe of X20CrMoV12.1 steel (German grade F12) after 23 years service.

Hu Zheng-Fei and **Yang Zhen-Guo**, Department of Materials Science, Fudan University, Shanghai 200433, P.R. China. Contact e-mail: zgyang@fudan.edu.cn.

2. Experimental Details

The investigated material is a section of 273OD × 26 mm thick main steam pipe of X20CrMoV12.1 steel, which had been in service for 23 years at 550 °C at a pressure of 13.7 MPa; its chemical composition is given in Table 1.

Both the foils and carbon extraction replicas for TEM study were prepared from the material. The foil samples for TEM were cut to about 0.3 mm thick from the sample, and then normally ground to about 60 μm and electropolished in a perchloric acid-alcohol solution at about –20 °C. Carbon extraction replicas were prepared for carbide identification with TEM and EDS. A small block of sample was polished and light etched in 5% nital, and then a thin carbon film was evaporated on it. The film was extracted by floating it in nital and supporting it on copper or nylon grids. The extraction replica supported on a nylon grid was only for investigation of the chemical composition of the carbides. The EDS spectra with nylon grid samples were obtained without extra peak from the grid background, which is convenient for later analysis.

The microstructural investigations were performed by analytical TEM. The TEM was carried out on both foil samples and carbon extraction replicas using a PHILIPS (Eindhoven, The Netherlands) CM200 TEM operated at 200 kV. Selected area diffraction (SAD) and x-ray microanalysis techniques were used to identify precipitation phases. As to the examina-

tion of the very fine precipitates, micro-beam diffraction was adopted. In this method, a diffraction pattern is formed by the finely converged electron beam illuminating only on a very small area of the specimen. In the present work, an electron beam of 60 nm was selected to study the very fine precipitates. An EDAX series DX-4 EDS (EDAX Int. Co., Mahwah, NJ) attached to the TEM was used to analyze the compositions of all the carbides. The x-ray spectra were recorded at a sample tilted 20°, with the converged electron beam illuminating only the isolated particles. The carbides were classified by morphologies, and more than 10 isolated particles of the same appearance were analyzed. The carbon element is not taken into account during the measurement of the compositions of the carbides because doing so would introduce a large error.

Table 1 Chemical Composition of the Examined Material, wt.%

C	Mn	S	P	Si	Cr	Mo	V	Ni	Cu
0.23	0.64	0.006	0.02	0.36	11.23	1.00	0.32	0.72	0.08

3. Results and Discussion

3.1 The Microstructure of the Examined Material

Figure 1 shows that the microstructure of the examined material is a typical tempered martensite with a high density of dislocations in the ferrite matrix, and there is no δ-ferrite observed. The most distinct microstructure character shown in Fig. 1 is the mass of substructure in the martensite laths, which developed during the long-term service of the pipe under a stress. Those substructures are formed by dislocations; a large number of dislocations gathered together to form subgrain boundaries and significantly reduced dislocation density in the matrix. Thus many low dislocation density regions are also seen.

Many of the precipitates can be seen in the examined material. Figure 1(b) is a TEM image of the corresponding carbon extraction replica from the same material. It clearly shows the distribution of the precipitating carbides; larger carbides are in prior austenite grain boundaries and in martensite lath boundaries, and the smaller carbides are dispersed in the matrix. A similar observation has been obtained in 12% Cr heat-resistant

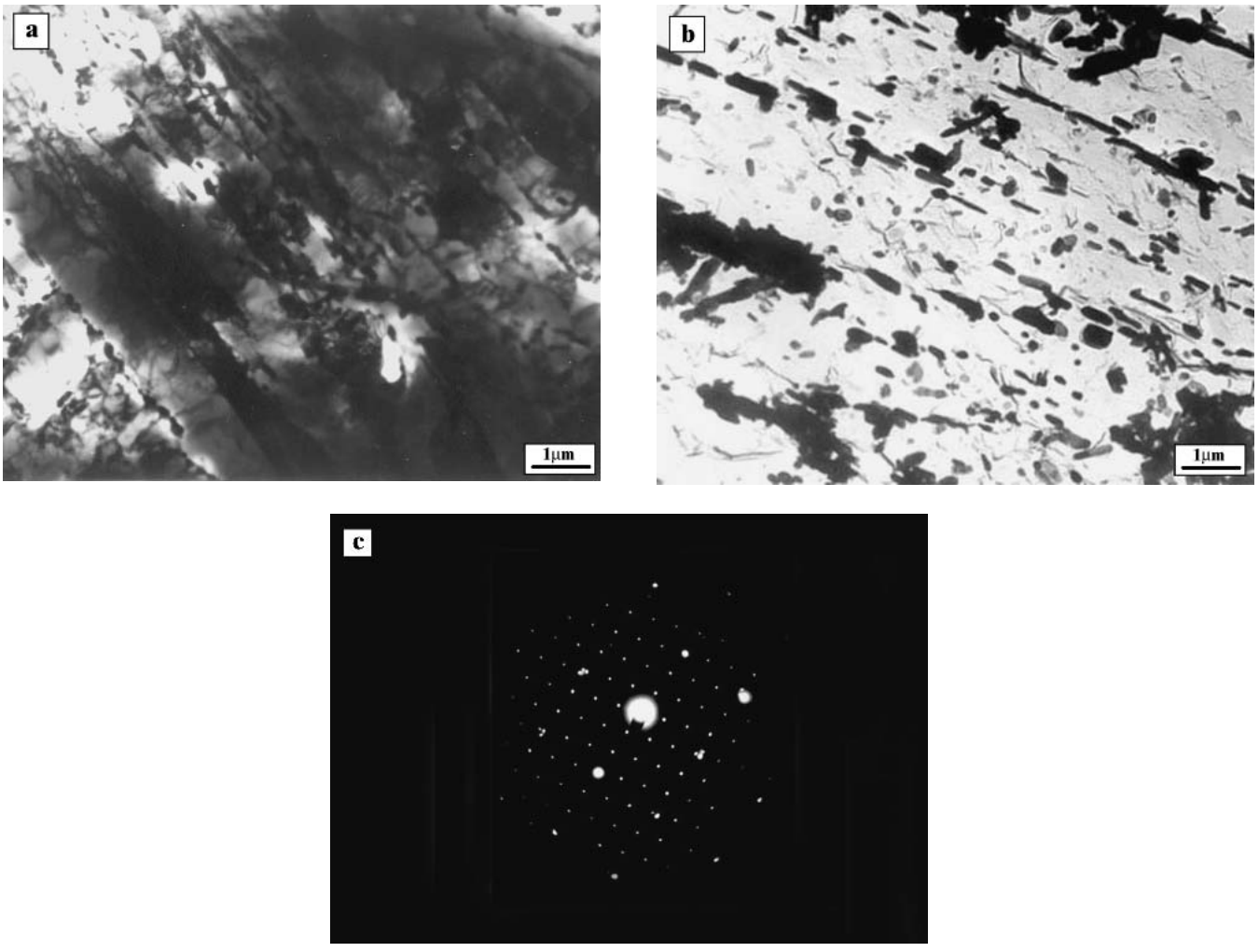

Fig. 1 TEM micrograph of **(a)** thin foil X20CrMoV12.1 steel service exposed for 23 years at 550 °C and **(b)** carbon extraction replica from the same sample; **(c)** SAD pattern of an interlath particle carbide

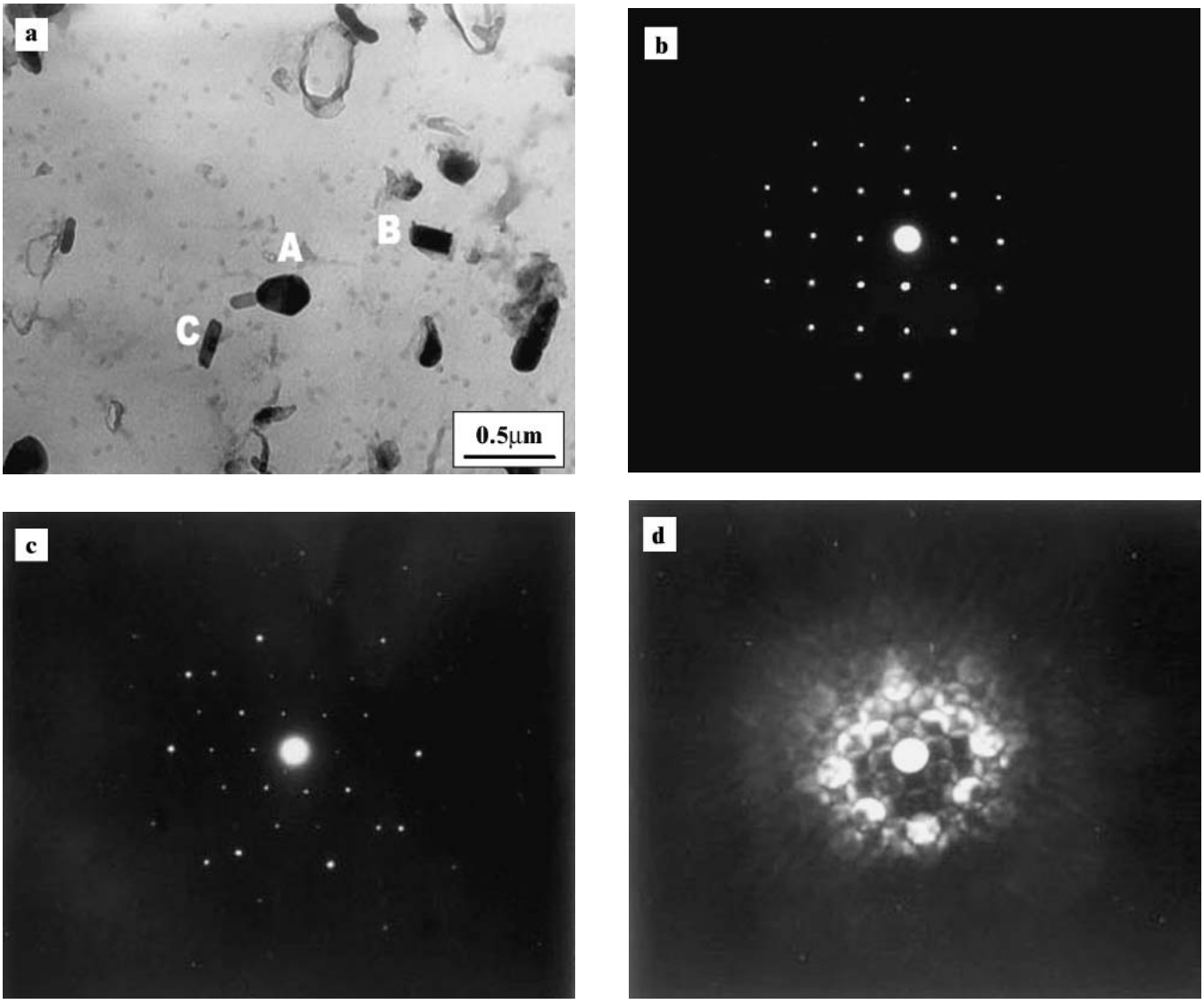

Fig. 2 **(a)** Fine carbides in different morphologies within the matrix; **(b)** and **(c)** diffraction patterns for spheroids; **(d)** diffraction patterns for rectangle plates (continued on next page)

steels by others.[7,9] The carbides, no matter whether in boundaries or in matrix, are in various shapes. More detailed investigations on the morphology and composition are discussed in the next section.

3.2 Identification of Carbide Phases

3.2.1 Carbides in Boundaries. The precipitating carbides in prior austenite boundaries and lath boundaries are well determined by selected area diffraction as $M_{23}C_6$. Figure 1(c) shows a SAD pattern of a particle of carbide in a lath boundary, and it is identified as $M_{23}C_6$ in [110] orientation. It is also shown that the $M_{23}C_6$ [110] direction is parallel with the [001] of ferrite matrix, which is identical with the relationship of Singhal and Martin.[10] Most of the carbides in prior austenite grains are in the form of an irregular spheroid with an average size in 0.33 μm. In contrast, most of the carbides in lath boundaries are in a plate-like morphology, with the long dimension about 0.35 μm on average, and the rest are in the form of an irregular spheroid. The intergranular and interlath carbides are coarsened distinctly, since their sizes are about twice those of the as-received condition measured by Eggeler[11] and Battaini et al.[12]

3.2.2 Carbides Within Matrix. Some much finer carbides can be seen within the matrix or in the martensite laths. Those fine carbides can be divided roughly into two categories by morphology; one a rectangular plate and another an irregular spheroid. Most of the intralath carbides are about 120 nm in size, and the smallest is less than 50 nm, which is about 50% larger than the statistical values measured by Ennis[13] and by Klimanek et al.[14] It is shown that those carbides are also coarsened. Carbides in intralaths are very fine, and in the foil sample it is almost impossible to get a clear diffraction spot pattern of the very small carbides from the thin specimens, due to the interference of the matrix. Therefore, carbon extraction replicas were used to determine the structure of the very fine

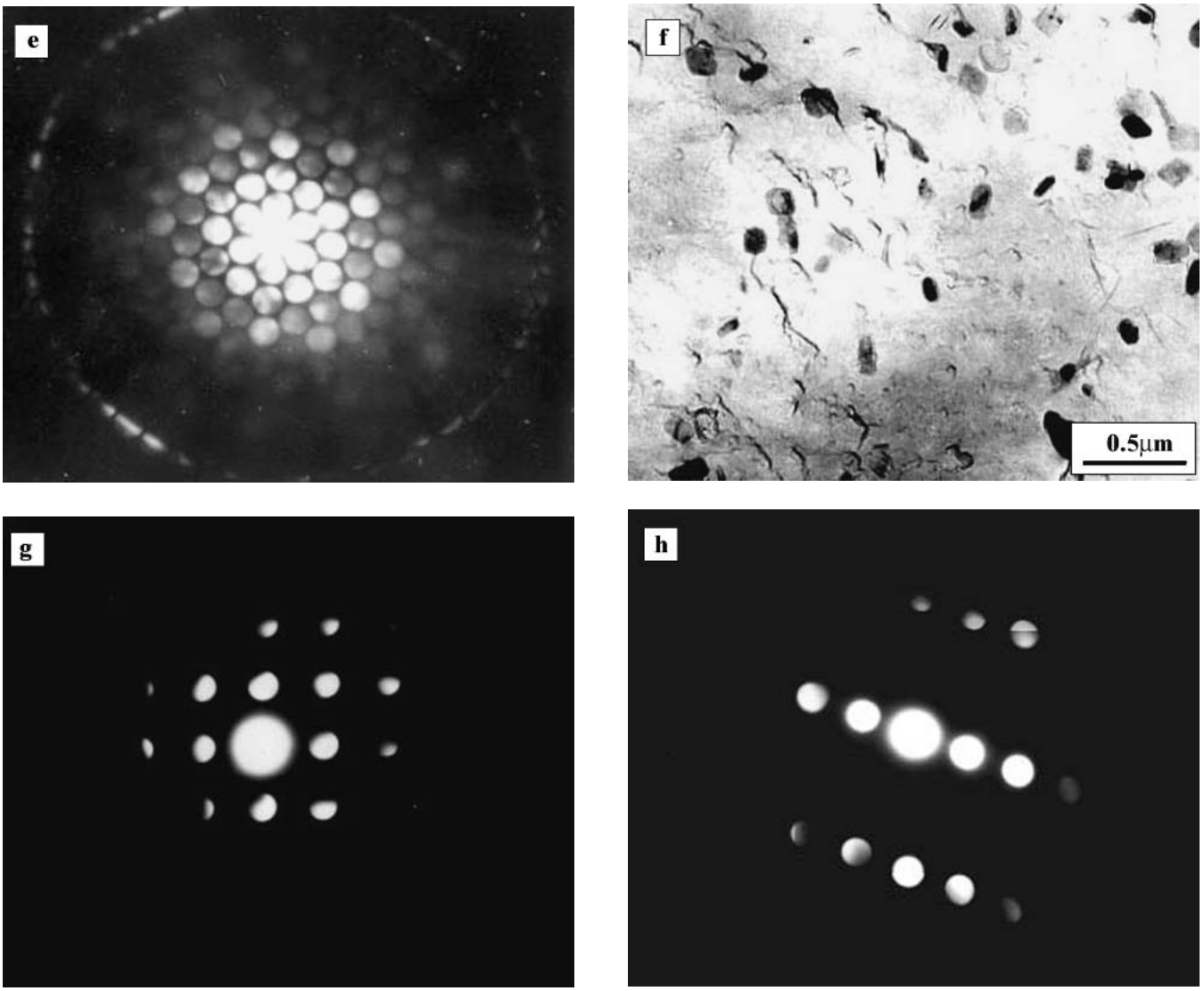

Fig. 2 cont. **(e)** diffraction patterns for rectangle plates; **(f)** fine V-rich carbides in clustering state, corresponding to diffraction patterns in **(g)** and **(h)**

carbides. In the extraction replicas, the carbides lost their original orientation with the matrix. To determine the crystallographic structure of the fine carbides, micro-beam diffraction studies were performed on the fine carbide particles in the matrix, and a diffraction pattern was taken with the very fine electron beam converged on the fine isolated carbide particles.

Figure 2(b) and (c) shows SAD diffraction patterns of an isolated spheroidal carbide particle (see Fig. 2a with letter A). They are indexed as face-centered cubic (fcc) structure with a lattice constant of 1.08 nm; the axes are [001] and [110], respectively. Another morphology of intralath carbides is a rectangular plate. One particle in such a shape is indicated by letter B in Fig. 2(a); Fig. 2(d) and (e) gives its micro-beam diffraction patterns, which are also indexed as fcc structure with a lattice constant of 1.07 nm, and the corresponding axes are [001] and [111]. It was determined that most of the carbides in the matrix in different morphologies are $M_{23}C_6$. The investigations of their compositions below will confirm this conclusion.

Except for the carbides mentioned above, some tiny carbides are in the uniform morphology of rectangular plate within the matrix. They are 100 nm or less; some finer than the $M_{23}C_6$ particles in varied shapes. In the EDS display they are identified as V-rich carbides. They are distributed in an isolated state as one particle in Fig. 2(a), indicated by letter B, or in cluster states shown in Fig. 2(f). Their distinct character is their TEM image, which have much light contrast; this means they are in a very thin sheet, only several nanometers in thickness. The isolated V-rich carbides are much larger, and those in the cluster state are smaller. The isolate V-rich carbides might be remnants from the as-received state, while those in clusters might be formed during long-term service. Figure 2(g) and (h) shows the micro-beam diffraction patterns of a V-rich particle in the cluster state; they are indexed as fcc structure of MX with a lattice constant of 0.41 nm, and the axes are [001] and [123].

Many types of carbides, including $M_{23}C_6$, M_7C_3, M_3C, M_2C, and MC, have been reported in 12%Cr steels; which types of carbides present are strongly dependent on the chemical compositions and heat treatment states of the examined

materials.[6,9,11] The microstructure investigation of 12CrMoV steels in the as-received heat treatment condition[7,15-16] showed that the finely dispersed M_2X and MX were observed within the matrix; M_2X is Cr-rich whereas MX is V-rich. The carbides in the X20CrMoV12.1 pipe steel after 23 years in service at 550 °C/13.7 MPa are mostly $M_{23}C_6$ in various morphologies, and no other carbides were found, except for some tiny V-rich carbides. It is obvious that the potential fine carbide phases, except $M_{23}C_6$, existing in the as-received heat treatment condition of the examined material mostly dissolved during the long-term service exposure at elevated temperature. This is similar to previous observations[7,9] that minor phases of M_2X and MX would dissolve after long-term creep exposure at elevated temperature with the coarsening of $M_{23}C_6$ carbides. Two different observations of the character of the precipitates in the present work were made: (1) the phenomena present in a special condition that the material is X20CrMoV12.1 pipe steel after 23 years in service at 550 °C/13.7 MPa; and (2) all the potential carbides are classified by morphology and extensively examined. The carbides with the same crystallographic structure as $M_{23}C_6$ in different appearances might be due to coarsening. The finding of tiny V-rich MC formed during long-term exposure at elevated temperature provides a good explanation of the phenomenon that the X20CrMoV12.1 steel did not soften during long-term service,[4] because V-rich carbides MX have a good coherent relationship with the matrix and have a strong hardening effect, both of which are beneficial for microstructural stability.

3.3 Chemical Composition of Carbides

3.3.1 Carbides in Boundaries. The chemical compositions of carbides in different morphologies were determined by an EDAX EDS from carbon extraction replicas supported on nylon grids, and thus the recording spectra contain no extra information. An EDS spectrum from a particle in a grain boundary is shown in Fig. 3(a). More than 10 spectra are recorded for the same morphology, and the compositions given below are average values of the quantitative analysis results. The compositions of spheroidal $M_{23}C_6$ carbides at grain boundaries contain 69 at.% Cr, 25 at.% Fe, 5 at.% Mo, and fractional V and Ni; plate particles at lath boundaries contain 65 at.% Cr, 28 at.% Fe, 2 at.% Mo, 3 at.% V, and fractional others. There is a slight difference between them in compositions, with the carbides at grain boundary containing a little more Mo and Cr, and the interlath carbides containing a little more V.

3.3.2 Carbides in Matrix. Most of the carbides in the matrix are also Cr-rich. The analysis EDS results reveal the compositions of spheroidal carbides with 70 at.% Cr, 20 at.% Fe, 8 at.% Mo, and fractional V and Ni. Those in rectangular plates are 70 at.% Cr, 20 at.% Fe, 3 at.% Mo, 6 at.% V, and fractional others. The spheroidal carbides contain more molybdenum, and the rectangular plate carbides contain much more vanadium.

It was found that most of the carbides in the material are Cr-rich, which confirmed that those carbides are not M_6C, but $M_{23}C_6$, because the former is Mo-rich and the latter Cr-rich.[9] The compositions of $M_{23}C_6$ are in general agreement with those of Strang and Vodarek.[7] The compositions of $M_{23}C_6$ carbides in the boundaries have a slight variance with those determined by Strang and Vodarek. This difference might be attributed to the difference of the compositions of the steels investigated.

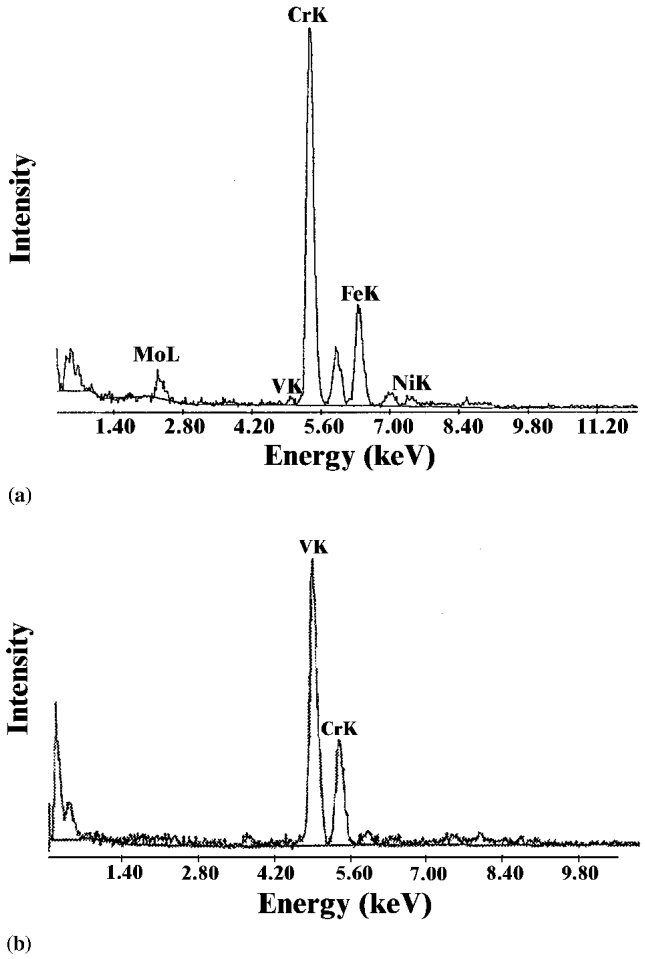

Fig. 3 Example of carbide EDS spectra from **(a)** a particle in a grain boundary and **(b)** a V-rich particle in the cluster state

3.3.3 V-Rich Carbides in Matrix. Several isolated V-rich carbides were found within the matrix. They contain 65 at.% V, 20 at.% Cr, and factional amounts of Fe, Ni, Mo, and Cu. The V-rich carbides in the cluster state contain 80 at.% V and 20 at.% Cr, which is obviously different than the isolated precipitates, and an EDS spectrum taken from one of them is shown in Fig. 3(b). This confirmed that the two states of V-rich carbides nucleated at different times: the isolated precipitates are remnants from the as-received state, and the cluster precipitates formed during long-term service.

An interesting result is the difference in composition of the $M_{23}C_6$ carbides, including the intergranular and interlath carbides, as well as the intralath carbides of different morphologies. In general, the irregular spheroidal carbides contain much more Mo and Cr relative to that in the plates, and the plates contain much more V. The most probable explanation is that all the $M_{23}C_6$ carbides in different states are coarsening, but at different rates; the irregular spheroidal carbides have coarsened more than those in plates. This suggestion is supported by previous investigations[6,11] that showed that the amount of Mo and Cr in the carbides increased slightly following aging or creep, and the intergranular carbides contained much more Cr

than the interlath carbides. Furthermore, the intergranular carbides coarsened faster than those in lath boundaries or within the matrix. It is well known that the carbide coarsening process is accompanied by particle coalescence and agglomeration, which markedly causes reduction of carbide particle volume density and reduces the precipitation strengthening mechanism. Meanwhile, the enrichment of solute in carbides during coarsening yields a contribution to depletion of the alloying elements into the matrix, which weakens the solid solution strengthening effect. So material degradation is very tight with the carbide coarsening.

4. Conclusions

1) In X20CrMoV12.1 pipe steel, which has been in service for 23 years at 550 °C at a steam pressure of 13.7 MPa, the carbides are in various morphologies and coarsened during exposure; in addition, the martensite structure undergoes degradation, and a substructure forms by dislocation reorganization.
2) The spheroidal carbides in prior austenite grain boundaries, the plate-like carbides in lath boundaries, and the much finer carbides within the matrix in different shapes were mostly $M_{23}C_6$. The compositions of those carbides vary with their morphology because they are coarsening at different rates during the long-term exposure at elevated temperature in service.
3) Very fine plate-like V-rich carbides formed after long-term service are identified as MC. These precipitates favor hardness maintenance and microstructural stability.

Refererences

1. S. Straub, M. Meier, J. Ostermann, and W. Blum: "Entwicklung der Microstruktur und der Festigkeit des Stahles X20CrMoV12.1 bei 823K Während Zeitstandbeans pruchung und Gl#369hung," *VGB Kraitwerkstechnik*, 1993, *73*(8), p. 744 (in German).
2. E. El-Magd, G. Nicolini, and M.A. Nasser: "The Influence of Prior Aging on Microstructure, Tensile Properties and Hot Hardness of Alloy 800HT," *Metall.,* 1996, *50*(11), p. 805.
3. D.B. Hahn and D.W. Bendick: "Erfahrungen aus der Zustandsbewertung eines FD- und HZÜ-Rohrleitungssystems aus dem Werkstoff X20CrMoV12.1 nach einer Bertriebszeit von über 180,000 h," *VGB Kraftwerkstechnik*, 2000, *11*, p. 85 (in German).
4. K. Borggreen and P.B. Mortensen: *Long-Term Properties of Fracture of X20CrMoV12.1*, The Danish Corrosion Center, Nov 1989.
5. R.B. Carruthers and M.J. Collins: "Carbide Transformations in Microstructurally Unstable Low Alloy Ferritic Steel," *Met. Sci.*, 1983, *17*(3), p. 107.
6. R.C. Thomson and H.K.D.H. Bhadeshia: "Carbide Precipitation in 12CrMoV Power Plant Steel," *Metall. Trans.*, 1992, *23A*(4), pp. 1171-79.
7. A. Strang and V. Vodarek: "Microstructural Stability of Creep Resistant Martensitic 12%Cr Steels" in *Microstructure of High Temperature Materials*, No. 2, A. Strang, J. Cawley, and G.W. Greenwood, ed., The Institute of Metals, London, UK, 1998, pp. 117-33.
8. P. Bianchi, P. Bontempi, A. Benvenuti, and N. Ricci: "Microstructural Evolution of P91 Steel After Long Term Creep Tests" in *Microstructure of High Temperature Materials*, No. 2, A. Strang, J. Cawley, and G.W. Greenwood, ed., The Institute of Metals, London, UK, 1998, pp. 107-16.
9. V. Vodarek and A. Strang: "Effect of Nickel on the Precipitation Processes in 12CrMoV Steels During Creep at 550," *Scripta Materialia*, 1998, *38*(1), p. 101.
10. L.K. Singhal and J.W. Martin: "The Nucleation and Growth of Widmannstätten M23C6 Precipitation in an Austenitic Stainless Steel," *Acta Metall.,* 1968, *16*(9), p. 1159.
11. G. Eggeler: "The Effect of Long-Term Creep on Particle Coarsening in Tempered Martensite Ferritic Steels," *Acta Metall*., 1989, *37*(12), p. 3225.
12. P. Battaini, D. Dangelo, G. Marino, and J. Hald: "Interparticle Distance Evolution on Steam Pipes 12% Cr During Power Plants' Service Time" in *Creep and Fracture of Engineering Materials and Structures*, *Proc. 4th Inter. Conf.,* B. Wilshire and R.W. Evans, ed., Apr 1990, The Institute of Metals, London, UK, pp. 1039-54.
13. P.J. Ennis, A.Z. Lipies, and A.C. Filemonowicz: "Quantitative Comparison of the Microstructures of High Chromium Steels for Advanced Power Stations" in *Microstructure of High Temperature Materials*, No. 2, A. Strang, J. Cawley, and G.W. Greenwood, ed., The Institute of Metals, London, UK, 1998, pp. 135-44.
14. P. Klimanek, K. Cyrener, C. Germain, K. Jenkner, U. Martin, O. Oettel, A. Ostwaldt, D. Ostwaldt, and W. Pantleon: "Flow Behaviour and Microstructure of the Heat-Resistant Steels X20CrMoV12.1 and X5NiCrTiAl32.20 (Alloy 800)" in *Microstructural and Mechanical Properties of Metallic High-Temperature Materials*, H. Mughrabi, ed., New York, NY, 1999, pp. 272-89.
15. A. Hede and B. Aronsson: "Microstructure and Creep Properties of Some 12% Chromium Martensitic Steels," JISI, 1969, *207*(9), p. 1641.
16. A. Strang and V. Vodareks: "Precipitation Process in Martensitic 12CrMoVNb Steels During High Temperature Creep" in *Microstructural Development and Stability in High Chromium Ferritic Power Plant Steels*, The Institute of Materials, London, UK, 1997, pp. 31-52.